Unsaturation and Liquefaction: Case Study of Dense Sand

K.H. Tran[1,6], S. Imanzadeh[1,2], S. Taibi[1], H. Souli[3], J.M. Fleureau[4], M. Hattab[5], and D.L. Dao[7]
[1] *Normandie Univ., UNILEHAVRE, UMR 6294 CNRS, LOMC, Le Havre, France*
[2] *Normandie Univ., INSA Rouen Normandie, Laboratoire de Mécanique de Normandie, Le Havre, France*
[3] *Ecole Nationale Supérieure de Saint Etienne, Laboratoire de Tribologie et and Dynamique des Systèmes, CNRS UMR 5513, Saint Etienne, France*
[4] *Université Paris-Saclay, CentraleSupélec, CNRS UMR 8579, Laboratoire de Mécanique des Sols, Structures et Matériaux, Gif-sur-Yvette, France*
[5] *Université de Lorraine, Laboratoire d'Etude des Microstructures et de Mécanique des Matériaux, CNRS UMR 7239, Arts et Métiers ParisTech, Metz, France.*
[6] *Thai Nguyen University of Technology, Thai Nguyen, Vietnam*
[7] *University of Transport and Communications, Hanoi, Vietnam*
E-mail: trankhaihoan@tnut.edu.vn

ABSTRACT: The main objective of this paper is studying the behaviour of dense RF Hostun sand subjected to dynamic loading in the triaxial apparatus. The samples with the same initial conditions (water content, void ratio) were prepared by the wet tamping method. After that, the samples were saturated, and then an effective cell pressure of 100 kPa was used to consolidate the sample. To study the liquefaction behaviour of sand, all the samples were subjected to dynamic deviator loading until liquefaction. The experiments show that the cyclic stress ratio needed to liquefy the sample was significantly affected by the saturation degree. All saturated samples were liquefied by the same level of deviator stress; however, the cycle numbers needed to liquefy the samples are different. The results suggest that besides the void ratio and the saturation degree, the sand liquefaction susceptibility may be affected by the different soil fabrics caused by sample preparation technique.

KEYWORDS: Hostun RF sand; Skempton parameter B; Cyclic loading, Liquefaction; Unsaturation.

1. INTRODUCTION

Soil liquefaction is a geo-phenomenon that often causes great damage to facilities. In common usage, liquefaction is usually related to saturated incoherent soils subjected to loading due to the increase of pore water resulting in the decrease of effective confining stress, and in the end, the soil behaves like a liquid. Liquefaction can be classified into three types (Robertson and Fear, 1996): flow liquefaction, cyclic liquefaction, and cyclic mobility. The two first types relate to the loose soils, and the last one relates to the liquefaction of dense soils. The most accepted criterion for liquefaction in laboratory tests is that the sample is liquefied if one of the following conditions appears: i) the increase of pore water pressure to cell pressure leads to the loss of effective confining stress (Seed and Lee, 1966); ii) axial strain in one cycle reaches 5% (Ishihara 1993).

Many studies have focused on the liquefaction of saturated soils, and it has been clearly understood (Castro G, 1969; Seed et al., 1982, etc.); however, recent studies have shown that liquefaction can be observed not only in saturated soil but also in unsaturated sandy soils. Tsukamoto et al. (2014) showed that the air bubbles could be found at 5m below the groundwater table, it means that perhaps most of the building structures are based on unsaturated soil layers. The theoretical study of Martin et al. (1978) predicted the effect of saturation degree on the cyclic liquefaction resistance of sands. Whereby the unsaturated sands can be liquefied, and a small change of saturation can cause a significant change in the cyclic stress ratio causing liquefaction. This finding has been confirmed by the laboratory results (Chaney, 1978; Yoshimi et al., 1989; Fourie et al., 2001; Tran et al., 2018). Mase et al., 2019 and some other authors carried out liquefaction tests on undisturbed samples, and they also made the similar conclusions. Mulilis et al. (1978) investigated the liquefaction of Monterey sand with the effect of Skempton's coefficient B, and they found that the resistance of sand does not change when the value of B is between 0.91 and 0.97. Tran et al. (2019) carried out tests on the unsaturated samples and had a conclusion that the sample with high relative density and in the unsaturated state can liquefy under cyclic loading. Della et al. (2011) demonstrated that the dilatancy and the contractancy of soils change when the Skempton's pore pressure coefficient B decreases; however, the influence is not the same for all soils. It depends on the soil type, initial density, and confining pressure.

Although laboratory studies on the effect of saturation degree have achieved some progress, it is necessary to have more studies to make clear the issues, such as the effect of saturation degree and the sample preparation on the liquefaction of sand in a very dense state. Unlike the samples in a medium-dense state, the very dense samples usually liquefy after a larger number of cyclic loading, especially when they are not fully saturated. Thus, the effect of sample preparation may not be clear in samples with a medium relative density but on the very dense samples. This paper presents five tests (Table 3) to study the behavior of RF Hostun sand, fine clean sand usually used in geotechnical laboratory tests in France. The first four experiments were carried out on fully saturated samples, while the last experiment was performed on the unsaturated samples. Through these tests, the influence of saturation degree and different soil fabrics caused by sample preparation are studied.

2. MATERIAL

The material is fine quartz sand (Hostun RF) from Sika Co. The sand with its microscope particle shape is shown in Figure 1, and the grain size distribution of the material is presented in Figure 2.

This material has the following parameters: specific gravity 2.65 g/cm^3, maximum grain size 0.6mm, minimum grain size 0.12 mm, and friction angle 400. Other parameters are shown in Table 1. Where D_{10}, D_{50}, and D_{60} are the particle size distributions of RF Hostun sand, *e* is the initial void ratio of the sample.

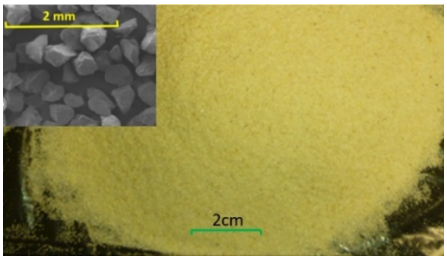

Figure 1. RF Hostun sand and its microscopic picture

Table 1 The parameters of RF Hostun sand

D_{50} (μm)	D_{10}	D_{60}	e_{max}	e_{min}
300	200	400	1.041	0.648

3. DYNAMIC TRIAXIAL APPARATUS

The apparatus used for dynamic triaxial tests were used in this study (Figure 3). The Dynamic (Cyclic) Triaxial Testing System 5 Hz/5 kN provided by VJ tech includes a dynamic controller to generate and control dynamic parameters, i.e., force, displacement, and pore water pressure. The cell pressure and back pressure are controlled by a Pneumatic Automatic Pressure Control (APC) device and a Hydraulic APC device, respectively. The pressure imposed by the Pneumatic APC is transmitted to the cell through an Air-Water Interface. This device's duty is to make the pressure more responsive and mellifluous. It includes a rubber ball embed in a cell. The pressure generator controls the air pressure inside the rubber ball instead of cell pressure directly. The specimen dimensions are 70 mm in diameter and 140 mm in high. The back pressure is applied to both the top and bottom of the sample, while the pore water pressure is measured only at the bottom of the sample. The displacement can be controlled by the axial displacement transducer or by the dynamic controller (this device makes and controls dynamic load)

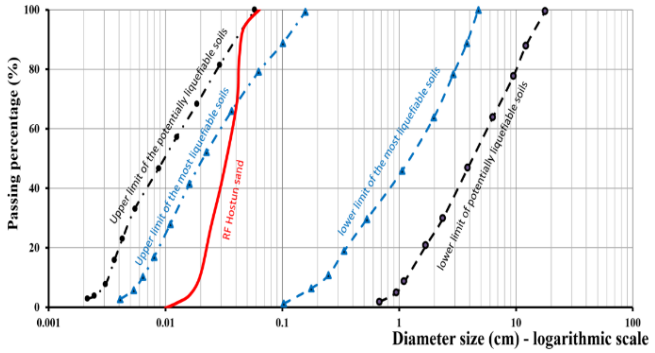

Figure 2 Comparison of the grain size distribution of Hostun RF sand to other liquefiable sands (Iwasaki 1986)

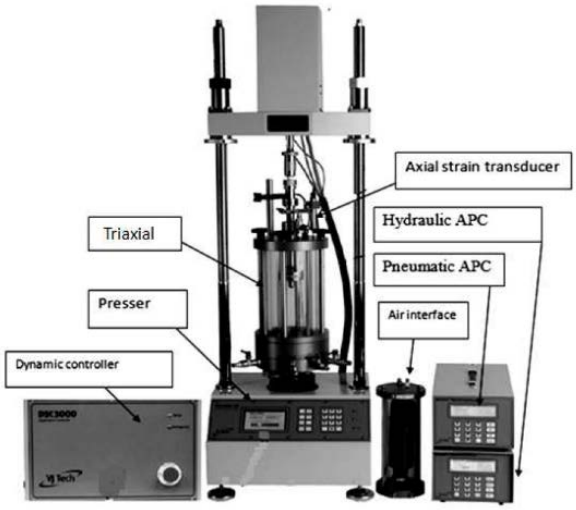

Figure 3 Triaxial dynamic testing apparatus

4 TEST PROCEDURE

4.1 Sample Preparation Using Moist Tamping

In the past, several researchers have pointed out the effect of sample fabric on the liquefaction potential of granular soil. Ladd (1974; 1977) was among the first attempts observing that the soil fabric affects significantly the cyclic shear strength behaviour of soil. These observations were confirmed by Mulilis et al. (1977). In addition to that, Mulilis et al. (1977) also concluded that the samples reconstituted by the wet tamping method are more nonuniform than the samples reconstituted by other methods and proposed an improvement for the wet tamping method. The wet tamping method was first proposed by Castro (1969), at that time, the samples reconstituted by this method was made from only one layer, thus, this method was also known as constant compactive effort method. In the improved wet tamping method, the samples were compacted layer by layer to reach the desired relative density. Mulilis et al. (1978) verified that the improved wet tamping method generates the samples more nonuniform than the constant compactive effort method proposed by Castro (1969); however, are less uniform than the samples reconstituted by the pluviation methods. The fabrics of the samples prepared by this method has been still being the great controversy. Vaid et al. (1999) showed that the wet tamping method does not simulate well the nature deposit fabrics. Ishihara (1993) suggested that the use of the wet tamping method was questionable. Dennis (1988) observed that the nonuniformity of the samples affects significantly the tests in stress - controlled condition but not for strain-controlled condition. On the other hand, many of the most important concept in liquefaction domain have been studied on the wet tamping prepared samples, for example the steady state (Poulos, 1981); the state parameter (Been and Jefferies, 1985).

In this study, the samples were prepared by the wet tamping method improved by Mulilis et al. (1977). Firstly, the sand was dried, and then a fixed quantity of water was added to have a mixture with the initial water content equal to 8%. This water content results in capillary forces between sand particles and allows reaching high density. The capillary forces are also useful in keeping the sample form stable after removing the split mould. The sample size is 70 mm in diameter and 140 mm high and initial void ratio of 0.73 corresponding to the relative density equal to 79%.

4.2 Sample Saturation and Skempton's Coefficient B Measurement

With the saturated tests, firstly, a cell pressure of 35 kPa had been applied, and after, the sample was circulated by de-aired water. The back pressure equal to 15 kPa was applied to the base of the sample; de-aired water flowed from the bottom to top and went out of the sample. With saturated tests, this process finished when there were not any air bubbles in the outlet pipe. After that, the cell pressure and back pressure were increased slowly to 770 and 750 kPa, respectively to dissolve the remaining air bubbles in the sample (Figure 4). In this process, the effective stress was kept equal to 20 kPa. With the unsaturated tests, the sample was circulated by de-aired water until reaching the desired saturation degree.

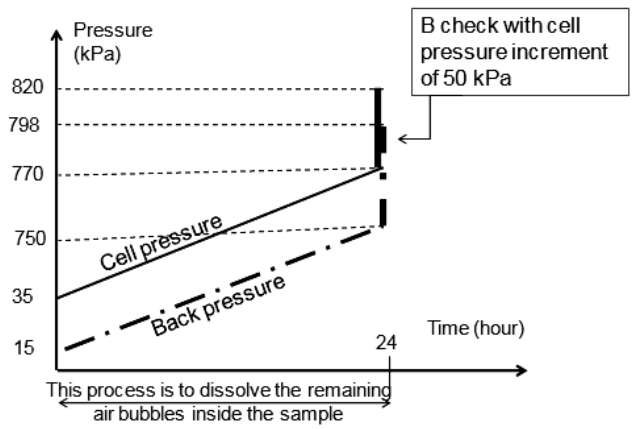

Figure 4 Cell and back pressure enhancement to dissolve the remaining air bubbles inside the sample

After the sample saturation process, Skempton's coefficient B value was used to estimate the saturation degree of the sample. To do this experiment, first, all the back pressure valves are locked. Thereafter, the cell pressure is increased. This increase in pressure results in an increase in the pore water pressure. The ratio between the measured pore pressure increases and the imposed cell pressure increase is defined as Skempton's coefficient B:

$$B = \frac{\Delta u_w}{\Delta \sigma_3} \quad (1)$$

where $\Delta\sigma_3$ and Δu_w are the imposed increment of confining stress and the resulting measured increment of pore water pressure, respectively.

Because water is incompressible compared to the soil skeleton, the sample is considered to be fully saturated if B = 1. The appearance of air bubbles with their compressibility makes smaller B value. In practice, a B between 0.95 and 0.97 is considered as a signal to indicate the full saturation of sandy soils due to some compliances of the test apparatus and sample compressibility (Chaney 1978, Jefferies 2016). To define the B of full saturation state, some experiments were carried out in our laboratory following the protocol: Firstly, cell pressure and back pressure are increased from 0 kPa and 20 kPa to 650 kPa and 670 kPa respectively to dissolve the air inside the sample (Figure 5). And then, when these pressures reach the target value, they are kept stable. Because of the dissolving of air bubbles into de-aired water, water from the Hydraulic APC (Figure 3) flows to the sample. The speed of this flow becomes lower and lower until there are not any air bubbles inside the sample and water stops moving from Hydraulic APC to the sample. At this time, the water volume measured by Hydraulic APC does not change (Figure 5). Lastly, a B check is applied to measure the B value of the full saturation state. B = 0.97 is obtained in our laboratory when the sample is completely saturated. This value was also used by some researchers, such as Benahmed (2001) and Arab et al. (2016), for RF Hostun sand as an indication of a full saturation state.

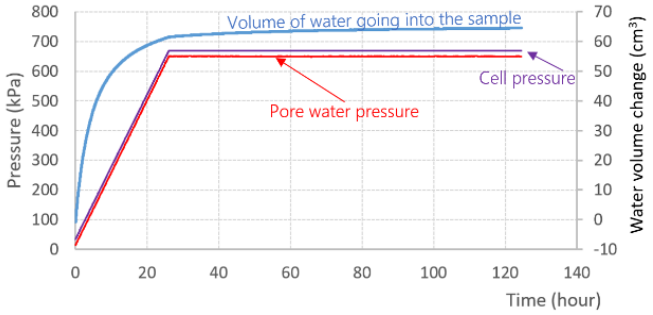

Figure 5 Air dissolves into de-aired water when pore water pressure and cell pressure ramp up.

Many studies have shown that the saturation degree is related to the Skempton's parameter B. Theoretically, the saturation degree can be modelled by Eq. (2). The relationship between B and Sr for RF Hostun sand is shown in Figure 6 (Tran et al. 2021)

$$B = \frac{1}{1+n\frac{K_s}{K_{aw}}} \quad (2)$$

where K_{aw} is calculated using Eq. (3) (Xia and Hu 1991)

$$K_{aw} = \frac{K_w}{1+(1-S_r)\left(\frac{K_w}{K_a}-1\right)} \quad (3)$$

where K_w and K_a are the bulk modulus of the water and air, respectively; n is the porosity of soil; K_s is the bulk modulus of soil skeleton. These parameters are shown in Table 2 (Tran et al., 2021).

From this calculation, the B value of 0.72 corresponds to the saturation degree Sr of 99.1%.

Table 2 Parameters for B-Sr modelling

K_w	K_a	K_s
2.23×10^6 kPa	143.8 kPa	15632 kPa

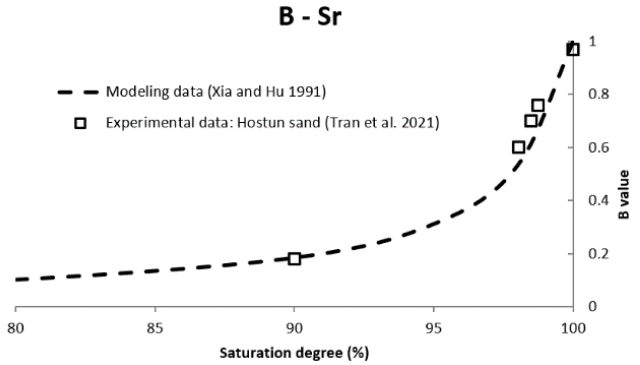

Figure 6 Relationship between saturation degree, Sr, and Skempton's parameter B for RF Hostun sand (Tran et al., 2021).

4.3 Isotropic Consolidation

To make the sample consolidated, firstly, all back pressure valves were closed, and thereafter the cell pressure was increased to have the difference of 100 kPa between the cell pressure and the back pressure (effective confining stress of 100 kPa). This results in the rising of pore water pressure. It takes some minutes to have the stability of effective confining stress. With saturated tests, because B ≈ 1, the effective confining stress before and after cell pressure increment was nearly equal, while there was a large difference for unsaturated experiments depending on the value of B (Eq. 1). After reaching the stability of pore water pressure, the back pressure valves were opened. The water went out of the sample through both ends due to the imbalance between the back pressure and the climbed-up pore water pressure. The cell pressure reduced gradually until, by the back pressure, the effective stress increased gradually and reached 100 kPa at the end of the process. The sample volume change during consolidation was measured by Hydraulic APC device, as shown previously in Figure 3.

Figure 7 shows the void ratio change due to the increase of the effective confining stress during the consolidation process. Tests 1 to 4 have Skempton's coefficient B ≈ 1, so all curves of these tests start at the same point where the initial effective consolidation stress is 20 kPa (This value is nearly equal to the effective confining stress during the sample saturation process). Test 5 has a B equal to 0.72. In other words, when measuring Skempton's coefficient B, the increasing of the cell pressure from 35 kPa to 100 kPa generates 52 kPa of the pore water pressure increment. At the end of the consolidation process, all tests have the same void ratio.

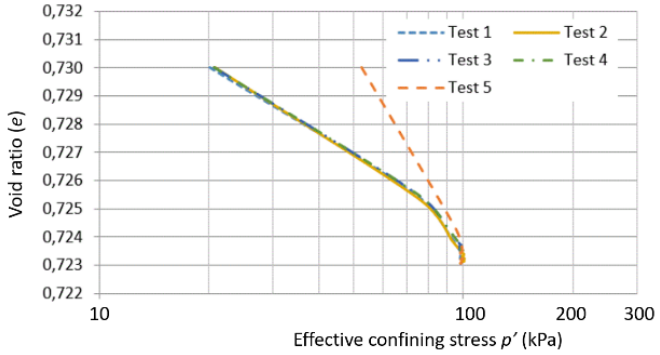

Figure 7 Void ratio in the function of effective consolidation stress

4.4 Dynamic Deviator Loading

The saw teeth form load with a frequency of 0.1 Hz, and 100 cycles were used to the top of the sample. With this frequency, it took ten seconds to finish a cycle of load, as shown in Figure 8.

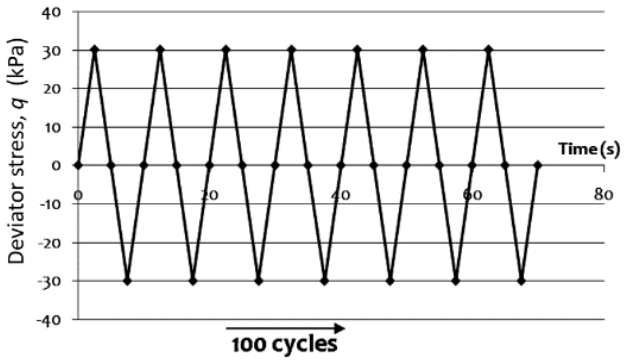

Figure 8 Cyclic deviator loading with CSR = 0.15

Cyclic stress ratio (CSR) is defined by using Eq. (4):

$$CSR = \frac{q^{c}_{max}}{2\sigma^{'}_{3c}} \quad (4)$$

where q^{c}_{max} is the amplitude of deviator cyclic stress, $\sigma^{'}_{3c}$ is the effective consolidation stress.

After 100 cycles of the first cyclic load case, if the sample is still not liquefied, the amplitude of cyclic deviator stress will be increased to have CSR of 0.2, 0.25, and 0.3 (Table 3). In case the sample shows the tendency of liquefaction, the test will continue with unchanged CSR, so the number of cycles of the final load case may be higher than 100 (Test 1).

Table 3 Definition of load case 1-4 with CSR

Load case	Load case 1	Load case 2	Load case 3	Load case 4
CSR	0.15	0.2	0.25	0.3

Table 4 presents the difference in the number cycle of the saturated tests (Test 1 to Test 4) and the increase of CSR when the saturation degree changes (Test 5). Tests 1 to 4 were performed with the same conditions, but the liquefaction occurred at significantly different numbers of cycles.

Table 4 Test information

Test	B	Sr (%)	Dr	CSR_{max}	Number cycles	
					Last load case	Total
1	0.97	100.0	79%	0.25	112	312
2	0.97	100.0	79%	0.25	22	222
3	0.97	100.0	79%	0.25	50	250
4	0.97	100.0	79%	0.25	72	272
5	0.72	99.1	79%	0.3	23	323

5. RESULTS

5.1 Cyclic Behaviour of Dense Saturated Sand

Four saturated dynamic tests with the same initial conditions were carried out (Test 1 to Test 4). After 100 cycles of the first load case and 100 cycles of the second load case with deviator stress equal to 30 kPa and 40 kPa, all samples were not liquefied or showed the signals of liquefaction. The CSR was increased to 0.25, corresponding to the deviator stress of 50 kPa. With this CSR, the samples of all tests were liquefied. There are two criteria for liquefaction as mentioned above: i) the effective confining stress drops to zero, ii) the axial strain $\varepsilon_a = 5\%$

Figure 9 shows, in general, the variation of deviator stress of test 1 when CSR = 0.25. At the beginning of the process, the deviator stress fluctuates between 50 kPa and –50 kPa. After 60 cycles, the deviator stress amplitude starts decreasing due to the building up of pore water pressure resulting in the loss of soil resistance. The test finished after 312 cycles. At the end of the process, the deviator stress is not stable at zero.

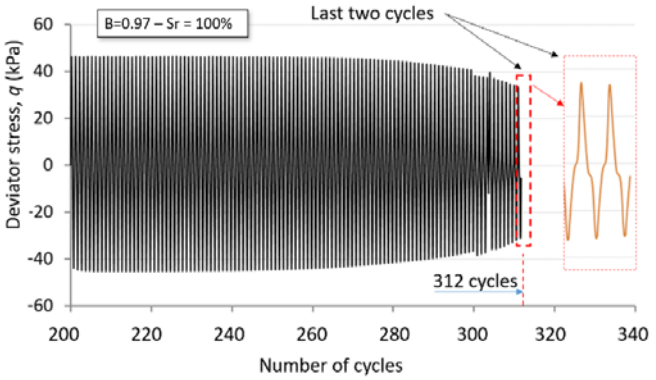

Figure 9 The deviator stress versus the number of cycles of test 1 when the CSR = 0.25

The development of pore water pressure due to the cyclic deviator stress is presented in Figure 10. The pore water pressure increases from 720 kPa to 800 kPa. The sample is liquefied, and the test is stopped after 312 cycles when maximal pore water pressure reaches cell pressure. In some last cycles, there is an appearance of the two-peak mechanism. In these cycles, there are two peaks of pore water pressure in each cycle of loading. It means that the number of times the sample changes its state from contraction to dilation or from dilation to contraction is two times as it is in the normal cycles.

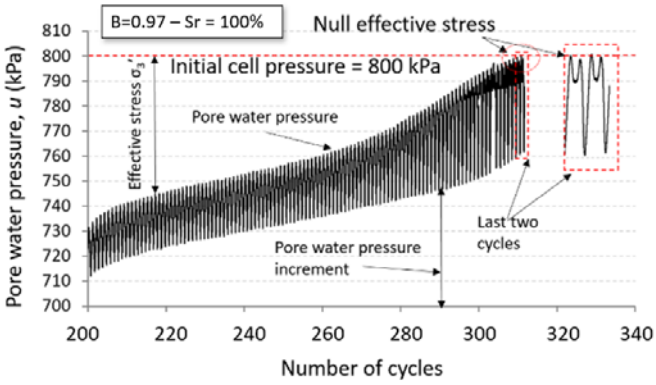

Figure 10 The Pore water pressure versus the number of cycles of test 1 when the CSR = 0.25 (B = 0.97-Sr = 100%)

Figure 11 presents the cyclic loading process of test 2 for load case 3 with CSR = 0.25. In the first five dynamic cycles, the deviator stress fluctuates between 50 kPa and -45 kPa, and then, the deviator stress amplitude starts reducing. The test stops after 222 cycles when the maximum and minimum values of the deviator stress amplitude are equal to 30 kPa and –30 kPa, respectively. Similar to the first test, at the end of the process, the deviator stress is not stable at zero.

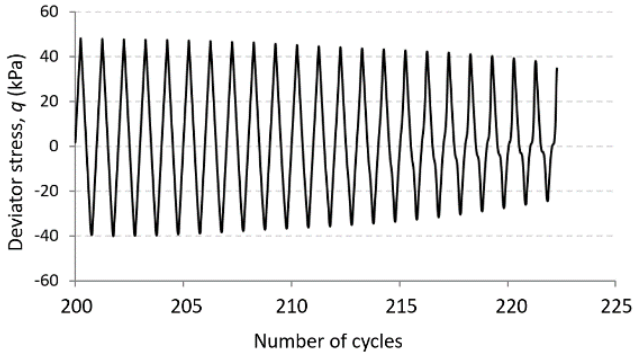

Figure 11 Deviator stress and pore water pressure of test 2 when the CSR = 0.25 (B = 0.97-Sr = 100%)

As shown in Figure 12, the pore water pressure caused by cyclic loading in test 2 fluctuates. Its amplitude reaches 800 kPa, the value of cell pressure, after 222 cycles.

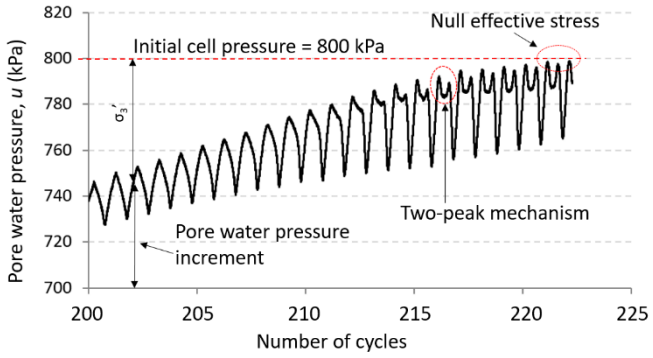

Figure 12 The pore water pressure versus the number of cycles of test 2 when the CSR = 0.25 (B = 0.97-Sr = 100%)

The liquefaction of test 2 is shown more obviously in Figure 13 by the results of the last ten cycles. It is clear that the pore water pressure increment builds up to the initial effective confining stress (100 kPa) in the 222nd cycle; however, the pore water pressure increment is only equal to the initial effective confining stress at some points, and it is possible to conclude that the liquefaction is cyclic mobility. At the end of the process, the deviator stress is approximately 35 kPa, lower than the initial value of 20 kPa.

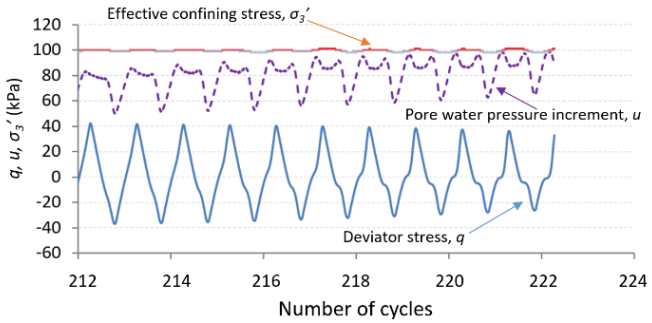

Figure 13 Deviator stress, pore water pressure, and cell pressure of the last ten cycles of test 2 (B = 0.97-Sr = 100%)

One of the parameters usually used to recognize liquefaction is the excess pore water pressure ratio. This ratio is calculated by normalizing the excess pore water pressure generated during un-drained cyclic loading for the effective consolidation stress as the following equation (Eq. 5):

$$r_u = \frac{\Delta u}{\sigma'_{3c}} \quad (5)$$

where Δu is the excess pore water pressure and σ'_{3c} is the effective consolidation stress.

The maximum possible value for r_u is 1.0 (or 100%), which occurs when the pore water pressure equals cell pressure or the effective confining stress equals zero, and the sample is considered to be liquefied. Figure 14 clearly shows the variation of r_u of test 2. This ratio fluctuates due to the change of deviator stress and finally equals to 1 after 222 dynamic cycles when the deviator stress is nearly 35 kPa.

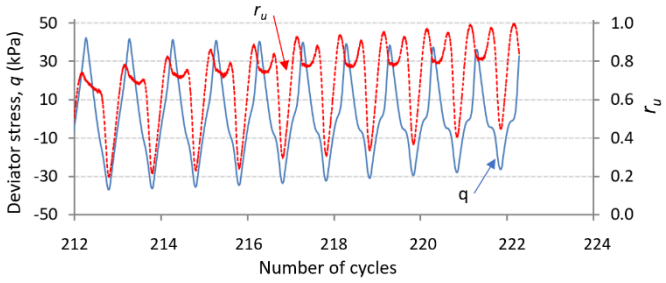

Figure 14 Excess pore water pressure ratio and cyclic deviator stress of the last ten cycles - test 2

Figure 15 presents the change of sample axial strain during cyclic loading of the last ten cycles of test 2 (with CSR = 0.25). The axial strain accumulates after each cycle of loading and equals to 1.7% after 222 cycles when deviator stress is equal to 35 kPa.

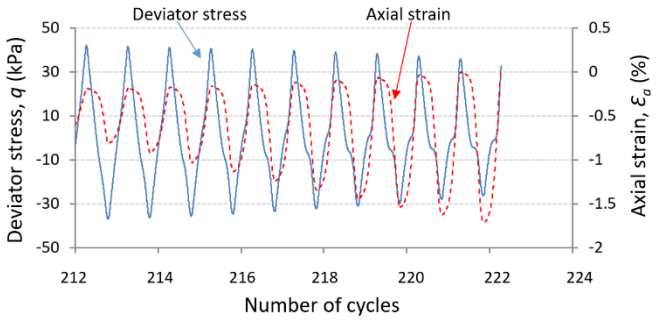

Figure 15 Axial strain and deviator stress versus number of cycles of the last ten cycles (CSR = 0.25) - test 2 (B = 0.97-Sr = 100%)

The relationship between axial strain and deviator stress is also surveyed and put on the view of Figure 16. The information observed from this Figure is that the axial strain increases quickly not at the moment when the deviator stress reaches maximum or minimum values but when this stress path passes zero. In each cycle, there are two times the axial strain develops sharply, and each time is in a different direction.

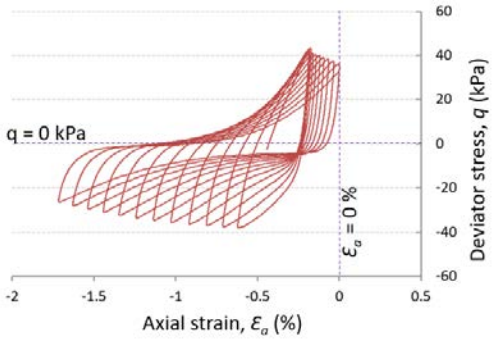

Figure 16 Axial strain in function of deviator stress of the last ten cycles - test 2 (B = 0.97-Sr = 100%)

Figure 17 presents more details about what happens with the cyclic mobility phenomenon. The form of this curve is the butterfly form. The q-p' curve approaches the failure criteria lines and fluctuates. As shown in this Figure, q is deviator stress and p' is effective mean stress. The slopes of the failure criteria lines can be calculated by using Eq. (6) and Eq. (7). The lines achieved from the test correspond to an effective friction angle $\phi_{scrit} = 37^0$. The deviator stress and effective mean stress increase each time the curve passes the phase transformation lines.

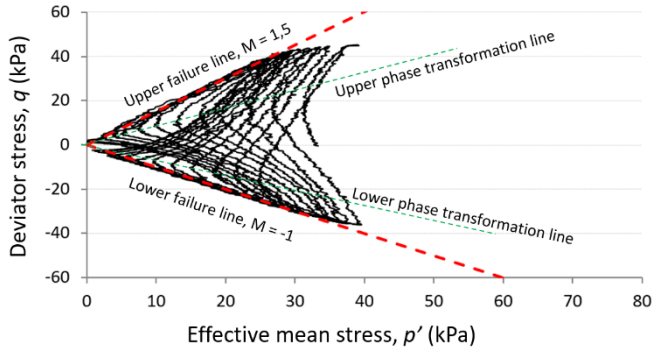

Figure 17 Deviator stress in the function of effective mean stress of the last ten cycles with CSR of 0.25 – test 2

$$M = \frac{6.\sin\varphi_{scrit}}{3-\sin\varphi_{scrit}} \quad \text{(Compression)} \qquad (6)$$

$$M = \frac{6.\sin\varphi_{scrit}}{3+\sin\varphi_{scrit}} \quad \text{(Extension)} \qquad (7)$$

where M is the slope of the failure criteria lines and $\phi_{scrit} = 37^0$ is the effective friction angle.

5.2 Effect of Unsaturation on The Cyclic Behaviour of Dense Sand

The liquefaction of unsaturated sand has been the subject of some researchers; however, not many studies have focused on the liquefaction of unsaturated soil in very dense states. Recently, Arab et al. (2016) investigated the effect of Skempton's parameter B on the liquefaction of RF Hostun in a medium-dense state. The result is that the decrease of B corresponding to the decrease of saturation degree results in the increase of liquefaction resistance of soil. The effect of saturation degree appears from the first cycle of cyclic loading. Unno et al. (2008); have conducted the strain-controlled cyclic loading on the samples of Toyoura sand with the relative density of 26% and 60% to study the pore air pressure and pore water pressure during cyclic loading. They found that the capillary suction is zero at the liquefaction state. With the same consideration and the same methodology, Tsukamoto et al. (2018); Mele et al. (2021) performed the tests on different types of sand and reached the same results. Another consideration for the liquefaction of unsaturated soil is the sample volumetric at liquefaction state. Okamura and Soga (2006) proposed the theoretical calculation base on the ideal gas law. In this study, they also showed that for the soil with saturation degree higher than 80%, the capillary suction is almost zero, and it is not necessary to measure the pore air pressure. Tran et al. (2021) presented the stepping cyclic loading method to liquefy the unsaturated samples in very dense state under stress-controlled conditions. Following their test protocol, the B value or saturation degree significantly affects both the number of cycles and the CSR needed to liquefy the samples. Tran et al. (2022) measured experimentally the sample volumetric strain at the liquefaction state. They also demonstrated that the conventional cyclic loading with constant CSR does not lead to the zero effective stress when the saturation degree is smaller than 95%. This is a limitation of the conventional cyclic loading with constant CSR when carried out on unsaturated samples.

When comparing test 5 to the tests from 1 to 4, the difference is only the degree of saturation. The sample was circulated by de-aired water, and B = 0.72 showed that it was not fully saturated. Like the saturated tests, the figures below present the results. In Figure 18, the deviator stress of the first seven cycles varies between 60 kPa and –50 kPa corresponding to CSR = 0.3. This value is larger than the maximum CSR of the three above-saturated tests. From the 8th cycle, the amplitude of the deviator stress starts declining. The sample liquefied after 323 cycles, and the slope of the failure criteria lines is the same with this of saturated tests as shown in Figure 19.

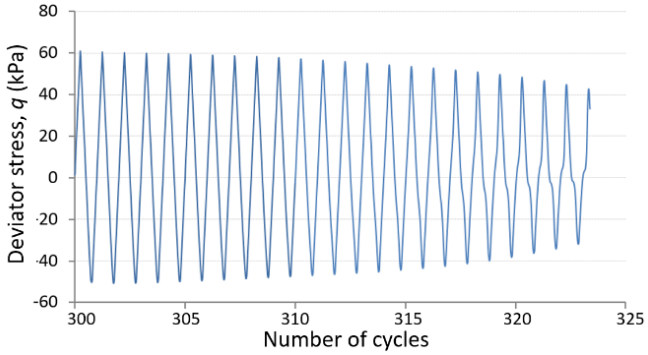

Figure 18 Cyclic deviator stress of test 5 with CSR = 0.3 (B = 0.72-Sr = 99.1%)

The relationship between deviator stress and effective mean stress is presented in Figure 19. It is mentioned that the slopes of the failure criteria lines in this Figure are equal to the slopes of failure criteria lines in Figure 17 (the failure criteria lines for the saturated tests with effective friction angle $\varphi_{scrit} = 37^0$). The deviator stress varies between 60 kPa and -50 kPa, while the effective mean stress decreases from almost 60 kPa to zero. When the curve contacts the failure criteria lines, it changes with the same slopes with these lines.

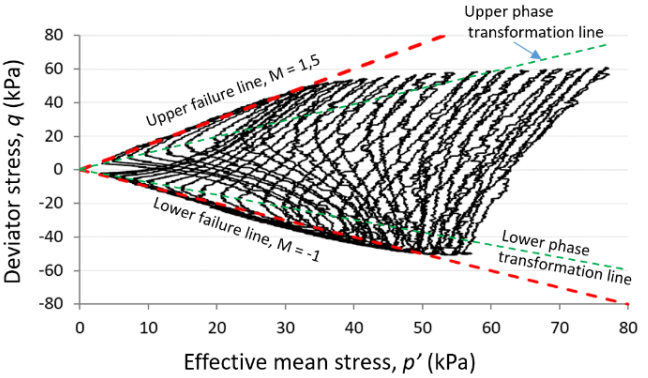

Figure 19 Deviator stress in the function of effective mean stress of the last ten cycles (initial CSR = 0.3) of unsaturated dynamic test 5.
(B = 0.72-Sr = 99.1%)

6. DISCUSSION

The unsaturated test in this study was carried out on the sample with saturation degree of 99.1%. For sandy soil, at this saturation degree, the air exists in soil porosity under air bubble form without contact with the grains, then the capillary suction is almost zero. Thus, the air pressure does not play any role in the strength of the material but plays a major role in the compressibility of the pore fluid composed by air – water mixture. Experimentally, it is not possible in this case to measure the air pressure inside these air bubbles. Some studies have demonstrated that when the saturation degree is higher than

80%, it is not necessary to measure the pore air pressure during cyclic loading of liquefaction tests (Okamura & Soga, 2006). In this study, it can be seen that the increase in the compressibility of the pore fluid expressed through the decrease of Skempton's parameter B affects the liquefaction potential by increasing both the number of cycles and the CSR.

The test 1 and 4 are fabricated using the same method, however, have different number of cycles at the liquefaction state. This can be explained due to the uncertainty of the micro fabric of the sample. The results also showed that the sample reconstitution in laboratory is not perfectively reproducibility. In Figure 20, it is clear that the sample prepared by the wet tamping method is not uniform. Inside the sample, the sand grains are densely distributed at some points and sparsely distributed at some points. From this observation, there are many areas existing in the sample with different relative densities, although the global void ratio or relative density of the sample is fixed. When subjected to cyclic loading, the loosest area contracts the most, causing an increase in pore water pressure. It means that the more nonuniform the sample is, the easier the sample is to liquefy. In our case, for saturated samples, these uncertainties lead to mean value of the total number of cycles of 264 to reach liquefaction with standard deviation of 33 and a coefficient of variation of about 12%.

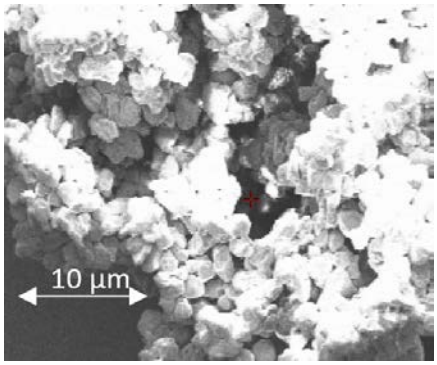

Figure 20 Microscopic photo of the RF Hostun samples prepared by wet tamping method (Benahmed, 2001)

7. CONCLUSIONS

This research paper presents a laboratory study of liquefaction on RF Hostun sand in both saturated and unsaturated states. Skempton's coefficient B = 0.97 was used to estimate the saturation degree of the sample. The saturated tests have Skempton's coefficient equal to B = 0.97, while the unsaturated test has a B of 0.72. The investigation shows that the sample with a relative density of 79% and Skempton's coefficient B higher than 0.72 can be liquefied under cyclic loading.

Comparing the results of saturated tests and unsaturated test, the conclusion is that the reduce of saturation results in an increase in the maximal dynamic cyclic stress ratio. The saturated samples are liquefied by cyclic loading with CSR of 0.25, while the unsaturated sample is liquefied under cyclic loading with CSR = 0.3. The CSR increases 0.05 (from 0.25 to 0.3) when Skempton's coefficient B reduces 0.27 (from 0.97 to 0.72). This can be explained that the air bubbles in unsaturated samples make the void between soil particles compressible, and then the pore water pressure increases less compared to saturated ones.

The slope of failure lines in saturated tests and unsaturated tests have the same values. It means that the effective friction angle is not affected by the saturation degree.

The results of saturated tests present that, although all samples have the same initial conditions and the maximal CSR, there is still a difference in the number of dynamic cycles causing liquefaction. This result leads to the conclusion that, with the sands in the dense state, besides the void ratio and the saturation degree, the different soil fabrics (caused by sample preparation technique: wet tamping) can have a significant role when evaluating the liquefaction susceptibility.

8. REFERENCES

Arab, A., Sadek, M., Benkhatir, M. (2016). "Saturation effect on behavior of sandy soil under monotonic and cyclic loading: a laboratory investigation". Geotechnical and Geological Engineering.

Been K, Jefferies M G (1985). "A state parameter for sand". Geotechnique, Vol. 35, No. 2, pp. 99–112.

Benahmed, N. (2001). "Comportement mécanique d'un sable sous cisaillement monotone et cyclique: application aux phénomènes de liquéfaction et de mobilité cyclique ». Thèses doctoral.

Castro, G. (1969). "Liquefaction of sands". Harvard University, Cambridge.

Chaney, R.C. (1978). "Saturation effects on the cyclic strength of sands". Proc., ASCE Special Conf. on Earthquake Engineering and Soil Dynamics, ASCE, New York, 342–359.

Della, N., Arab, A., Belkhatir, M. (2011). "Static liquefaction of sandy soil: an experimental investigation into the effects of saturation and initial state". Acta Mech 218(1–2):175–186.

Dennis, N. D., (1988). "Influence of specimen preparation techniques and testing procedures on undrained steady state shear strength, advanced triaxial testing of soil and rock", ASTM STP 977, R. T. Donaghe, R. C. Chaney, and M. L. Silver, Eds., ASTM, Philadelphia, pp. 642–654.

Fourie, A., Hofmann, B., Mikula, R., Lord, E., and Robertson, P. (2001). "Partially saturated tailings sand below the phreatic surface". Geotechnique, 51(7), 577–585.

Ishihara, K. (1993). "Liquefaction and flow failure during earthquakes". Geotechnique 43, 351-415.

Iwasaki T. (1986). "Soil liquefaction studies in Japan (state of the art). Soil Dynamics and Earthquake Engineering" 5(1): 2-68. doi: 10.1016/0267-7261(86)90024-2

Jefferies, M., Been, K. (2016). "Soil liquefaction – a critical state approach". CRC press book. Taylor and Francis Group, 472.

Ladd, R. S. (1974). "Specimen preparation and liquefaction of sand", J. Geotech. Engrg. Div., Vol. 100, No. GT10, pp. 1180–1184.

Ladd, R. S. (1977). "Specimen preparation and cyclic stability of sands," J. Geotech. Engrg. Div., Vol. 103, No. GT6, pp. 535–547.

Mulilis, J. P., Seed, H. B., Chan, C. K., Mitchell, J. K., and Arulanandan, K. (1977). "Effects of sample preparation on sand liquefaction". J. Geotech. Engrg. Div., Vol. 103, No. GT2, pp. 91–109.

Mullilis, J.P., Townsend, F.C., Horz, R.C. (1978). "Triaxial testing techniques and sand liquefaction". ASTM STP 654 Dyn Geotech Test, 265–279.

Martin, G.R., Finn, W.D.L., Seed, H.D., (1978). "Effects of system compliance on liquefaction tests". J Geotech Eng Div 104(4):463–479.

Mase, L.Z., Likitlersuang, S., Tobita, T., (2019). "Cyclic behaviour and liquefaction resistance of Izumio sands in Osaka, Japan", Journal Marine Georesources & Geotechnology, Volume 37, 2019 - Issue 7, https://doi.org/10.1080/1064119X.2018.1485793

Mele, L., Chiaradonna, A., Lirer, S., Flora, A. (2020.) "A robust empirical model to estimate earthquake-induced excess pore water pressure in saturated and non-saturated soils". Bulletin of Earthquake Engineering, 1-29.

Okamura, M., Soga, Y. (2006). "Effects of pore fluid compressibility on liquefaction resistance of partially saturated sand". Soils Found. 46 (5), 695-700.

Poulos, S.J., (1981). "The steady state of deformation". Journal of the Geotechnical Engineering Division, ASCE, 107(5), 553–562.

Seed, H.B., Idriss, I.M. (1982). "Ground motion and soil liquefaction during earthquake", Berkeley, University of California.

Seed, H.B., Lee, K.L. (1966). "Liquefaction of saturated sands during cyclic loading. journal of the soil mechanics and foundations division", ASCE 92, 105-134.

Tsukamoto, Y., Kawabe, S., Matsumoto, J., Hagiwara, S. (2014). "Cyclic resistance of two unsaturated silty sands against soil liquefaction". Soils and Foundations.

Tran, K.H., Imanzadeh, S., Taibi, S., Souli, H., Fleufeau, J.M., Bouchemelia, S., Pantet, A. (2018). "Cyclic behavior of unsaturated Hostun sand". The 4th International Conference Unsaturated Soils & Sustainable Construction UNSAT, Oran – Algeria.

Tran, K.H., Imanzadeh, S., Taibi, S., Souli, H., Fleufeau, J.M., Pantet, A. (2018). "Some aspects of the cyclic behavior of quasi-saturated sand". 36èmes Rencontres Universitaires de Génie Civil de l'AUGC. France.

Tran, K.H., Imanzadeh, S., Taibi, H. Souli, Fleureau, J.L, Hattab M, Luong N.H.P. (2019). "Effect of unsaturation on the liquefaction of soil: case study of dense fine clean sand". The 3rd Int. Conf. on Transport Infrastructure & Sustainable Development (TISDIC 2019), Da Nang - Vietnam.

Tran, K.H., Imanzadeh, S., Taibi, S., Dao, D.L. (2019). "Liquefaction behaviour of dense sand relating to the degree of saturation". The 4th International Conference on Geotechnics for Sustainable Infrastructure Development (GEOTEC HANOI), Hanoi - Vietnam.

Tran, K.H., Imanzadeh, S., Taibi, S., Souli, H., Fleureau, J.M., Hattab, M. (2021). "Effect of saturation on liquefaction potential and residual strength: laboratory investigation". European Journal of Environmental and Civil Engineering https://www.tandfonline.com/doi/full/10.1080/19648189.2021.1999333

Tran, K.H., Imanzadeh, S., Taibi, S., Souli, H., Fleureau, J.M., Hattab, M. (2022). "Liquefaction of unsaturated soils- Volume change and residual shear strength". European Journal of Environmental and Civil Engineering. https://doi.org/10.1080/19648189.2022.2075471

Tsukamoto. Y., (2018). "Degree of saturation affecting liquefaction resistance and undrained shear strength of silty sands". Soil Dynamics and Earthquake Engineering, https://doi.org/10.1016/j.soildyn.2018.04.041

Unno, T., Kazama, M., Uzuoka, R., (2008). "Liquefaction of unsaturated sand considering the pore air pressure and volume compressibility of the soil particle skeleton". Soils and Foundations, Volume 48, Issue 1, February 2008, Pages 87-99. https://doi.org/10.3208/sandf.48.87.

Vaid, Y.P., Sivathayalan, S., Stedman, D. (1999). "Influence of specimen-reconstituting method on the undrained response of sand". Geotech. Test. J., Vol. 22, No. 3, pp. 187–195.

Xia, H., Hu, T. (1991). "Effects of saturation and back pressure on sand liquefaction". J Geotech Eng 117(9):1347–1362.

Yoshimi, Y., Tanaka, K., Tokimatsu, K. (1989). "Liquefaction resistance of partially saturated sand". Soils Found, 29(3), 157–162.

Robertson, P.K., and Fear, C.E. (1996). "Soil liquefaction and its evaluation based on SPT and CPT, Liquefaction Workshop", January 1996.